Powder Technology 274 (2015) 284–288

Contents lists available at ScienceDirect

Powder Technology

journal homepage: www.elsevier.com/locate/powtec

Short communication

Investigation of granular impact using positron emission particle tracking

J.O. Marston [a,*], S.T. Thoroddsen [b]

[a] Department of Chemical Engineering, Texas Tech University, Lubbock, TX 79409-3121, USA
[b] Division of Physical Sciences and Engineering, King Abdullah University of Science and Technology, Thuwal, 23955-6900, Saudi Arabia

ARTICLE INFO

Article history:
Received 7 October 2014
Received in revised form 7 January 2015
Accepted 18 January 2015
Available online 26 January 2015

Keywords:
Granular impact
Fluidisation
PEPT

ABSTRACT

We present results from an experimental study of granular impact using a combination of high-speed video and positron emission particle tracking (PEPT). The PEPT technique exploits the annihilation of photons from positron decay to determine the position of tracer particles either inside a small granular bed or attached to the object which impacts the bed. We use dense spheres as impactors and the granular beds are comprised of glass beads which are fluidised to achieve a range of different initial packing states. For the first time, we have simultaneously investigated both the trajectory of the sphere, the motion of particles in a 3-D granular bed and particles which jump into the resultant jet, which arises from the collapse of the cavity formed by the impacting sphere.

1. Introduction

Granular impact is a fundamentally important topic in many applications, especially crater formations, which are ubiquitous on the surface of planets. Such craters, formed in hypervelocity impacts can be scaled in a similar fashion to those seen in laboratory experiments, whereby the crater diameter scales with the impact energy to the power $\frac{1}{4}$, i.e., $D_{crater} \sim E^{1/4}$ [1].

Laboratory experiments invariably involve the impact of dense projectiles onto loosely packed, dry granular beds. In such circumstances, the initial stages of impact can exhibit fluid-like behaviour, in the form of an ejecta sheet [4,5], sinking into the loose bed [3,7] and eventually a jet, shown in Fig. 1, resulting from the hydrostatic collapse of the cavity behind the projectile [6,9,11].

The above-surface events are readily observed, whilst the subsurface motion of the projectile within the bed and the motion of the bed itself are more difficult features to capture. This has previously only been achieved for the projectile using a tether [3,13,14] or with the use of X-ray tomography [9,10]. In the latter, X-ray imaging allowed the determination of changes in local packing fractions. In this communication, we report the use of positron emission particle tracking (PEPT) in granular impact to simultaneously track the motion of the projectile within a granular bed and the motion of individual particles in the bed.

2. Experimental methods

The PEPT technique exploits the decay of a radioisotope, which is incorporated into a tracer particle. During the decay, a positron is emitted and annihilates with an electron thus releasing back-to-back gamma-rays. The gamma rays are detected using positron cameras and thus the location of the tracer particle can be triangulated to within approximately 2 mm at an acquisition rate of over 10 kHz (see [2,8]). The PEPT technique has been documented in many prior studies, including applications to granular flows (e.g., [12]). In our experiment, the tracer particles used were aluminium oxide particles with diameters approximately 100 μm, chosen to match the size of the glass beads used in the granular bed (75–125 μm). The beads were poured into a cylindrical container 7 cm in diameter, whilst the projectile, a steel sphere was 2 cm in diameter. Due to the geometrical constraints of the setup ($D_{cyl}/D_0 = 3.5$), there will be wall effects. However, as in previous work [4,5], this effect is constant throughout the experiments so that we can neglect this aspect in our analysis. Three reproducible packing fractions, $\phi \approx 0.55$, 0.60 and 0.62 were achieved in this study by first fluidising the entire bed, then reducing the inlet air flow to the desired level. The sphere was released using an electromagnet positioned directly above the centre of the granular bed. A tracer particle was attached to the top of the sphere using adhesive tape, whilst multiple tracers were also placed in the bed. As such, the initial location of the tracer particles in the bed was random. A typical impact event is shown in Fig. 1, taken from a high-speed video sequence. Both the ejecta and jet, which arise from the collapse of the cavity, are seen. The jet, in particular, is a feature we focus on herein.

3. Results

Fig. 2(a) plots sphere trajectories within the granular bed (outlined in blue) for three different packing fractions. The sphere was tracked from approximately 100 mm above the surface of the bed until it came to rest. The bottom of the line plots indicates where the sphere

* Corresponding author. Tel.: +1 806 834 7012.
E-mail address: jeremy.marston@ttu.edu (J.O. Marston).

http://dx.doi.org/10.1016/j.powtec.2015.01.033
0032-5910/

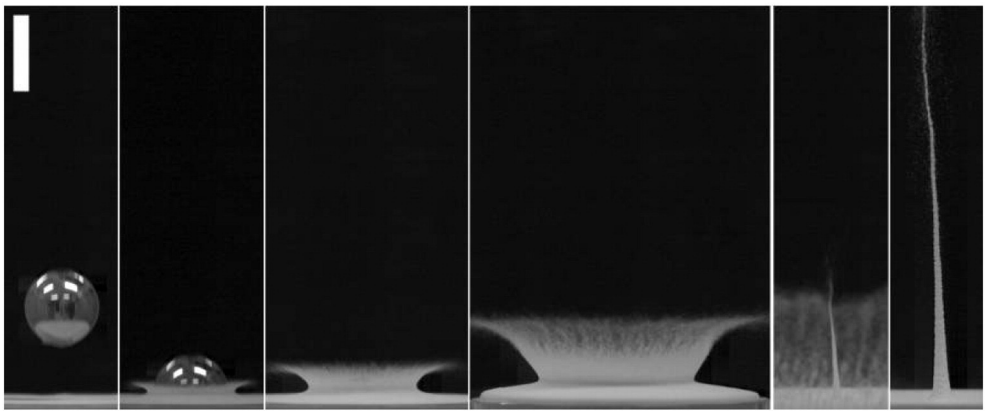

Fig. 1. Image sequence from a high-speed video clip of a 20 mm steel sphere impacting onto a bed of glass beads. The times from impact are $t = -10, 5, 10, 30, 100$ and 180 ms. The scale bar is 2 cm.

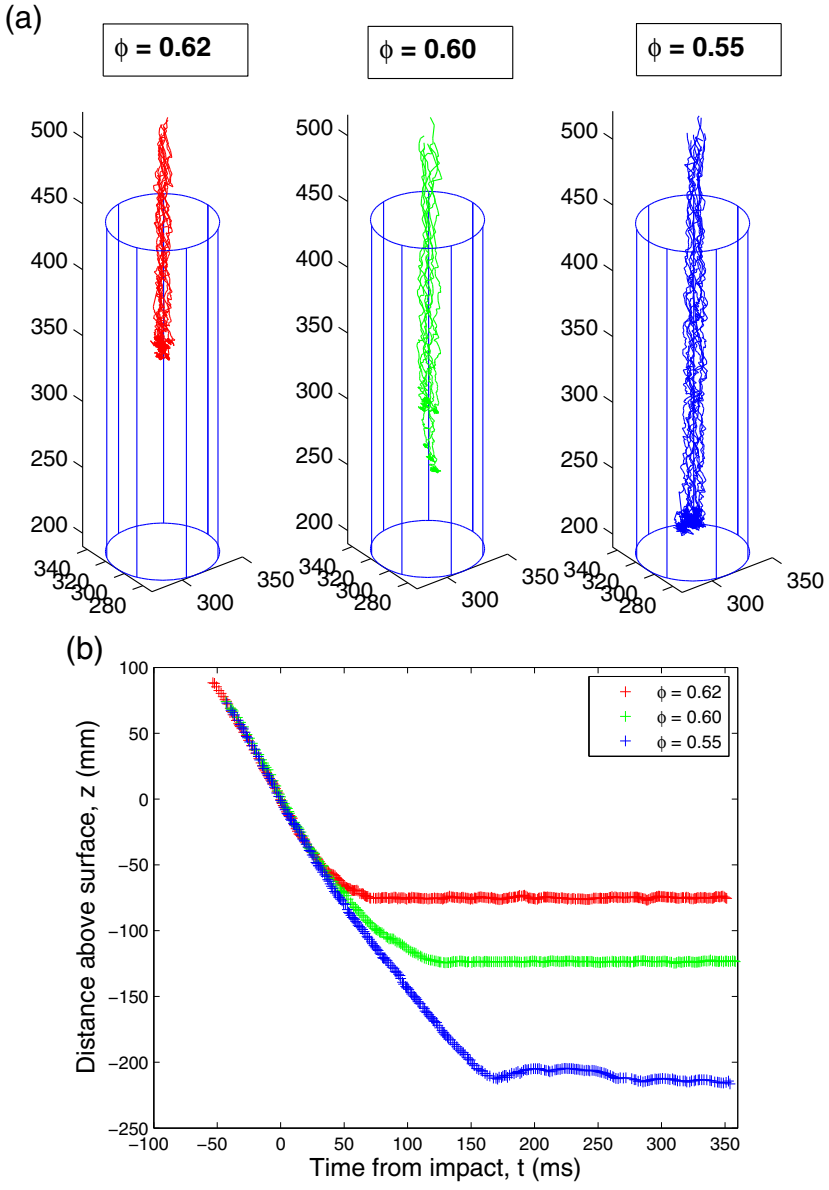

Fig. 2. (a) Ball trajectories determined by PEPT with the tracer particle attached to top of sphere. The three plots correspond to the three different initial bed conditions. The blue lines depict the edge of the cylinder filled with the granular media. (b) Depth of sphere centre vs. time curves for individual realisations from each of the three initial bed conditions. The blue data points, for the lowest packing fraction, show that the ball hits the bottom of the cylinder and exhibits a small bounce. In all cases $V_0 = 1.81$ m/s, $D_0 = 20$ mm, $Fr = 34$. (For interpretation of the references to colour in this figure legend, the reader is referred to the web version of this article.)

motion was arrested and, as expected, the sphere motion was arrested sooner for the highest packing fraction $\phi = 0.62$ than for the lower packing fractions $\phi = 0.6$ or $\phi = 0.55$. Fig. 2(b) plots the vertical distance from the surface versus time from impact for a typical impact for each of the packing fractions. The depths at which the spheres come to rest are evident here, with $z_{stop} \approx -75$ and -125 mm for $\phi = 0.62$ and 0.6, respectively. For the lowest packing fraction, $\phi = 0.55$, the sphere reaches the bottom of the container and exhibits a small bounce before settling.

Given the data acquisition rates of approximately 10 kHz, the error in the location is estimated to be within ± 2 mm [2], which gives us reasonably accurate data of the sphere trajectory. Note that a tether could produce much more accurate data in terms of displacement, but has only been used for vertical impacts, whereas the PEPT technique has the potential to be implemented in oblique impacts as well.

Fig. 3 plots both the jet height above the surface and the sphere depth below the surface against time from impact. The three cases shown are for the same experimental conditions as Fig. 2. We find that the jet emergence time, when the jet can first be seen above the initial surface of the bed, is approximately constant for all three bed conditions with $t_{jet} = 76 - 84$ ms. For $\phi = 0.62$, shown in (a), the sphere has just reached its final position when the jet emerges so that the entire jet motion above the surface occurs *after* the sphere is at rest. In contrast, for the lower packing fractions in (b) and (c), the sphere is still in motion as the jet emerges; In (c), the jet travels 150 mm during the 60 ms interval that we track the tip, whilst the sphere travels approximately 80 mm. Assuming a linear motion, i.e., constant speed, during the first few frames after the jet emerges, we estimate the speeds of the jet as $V_{jet} = 2.13$, 2.3 and 2.66 m/s for (a), (b) and (c) respectively, leading to normalised speeds $V_{jet}/V_0 = 1.18$, 1.28 and 1.48. In Fig. 4(a), the initial jet speeds from multiple repeat trials are plotted as a function of the initial bed packing fraction, showing a higher degree of variance for the low packing fraction compared with the two higher packings. This was also observed in Marston et al. [6] for similar geometries and grain size and is believed to be due to the influence of the superficial gas velocity in the bed, but has yet to be explained conclusively. Fig. 4(b) shows the final depth of the sphere versus packing fraction, indicating a rapid decrease as the packing fraction increases towards the close packing limit ($\phi \approx 0.64$). The error bars in this plot are due to a confluence of the error in the PEPT measurements and in the initial packing state.

Fig. 5 indicates the trajectories of multiple particles from repeat experiments (5 particles in each of 3 experiments) for the lowest packing fraction, $\phi = 0.55$. In Fig. 5(a), we plot the position versus time (shown by the colour scale on the right), where we begin recording prior to the sphere impact ($t = 0$). The central lines indicate the sphere motion, whilst the discrete points indicate particles randomly scattered in the bed. The initial and final locations of the particles in the bed (in the XY-plane) are shown in Fig. 5(b), with one particular particle showing a large displacement, which was the result of being incorporated into the ejecta during the early motions. The remainder of the particles exhibits only a small displacement. This is surprising given that some of particles were initially located directly in the path of the sphere (denoted by the black circle in Fig. 5(b)) and may be explained by considering the flow of grains radially outward and upward as the sphere passes, then settling back towards the centre after the sphere has passed.

Fig. 6 shows the vertical displacements of 3 particles tracked simultaneously during the impact and jetting process. In this realisation, one particle is attached to the sphere, one is located near the bottom of the bed and one particle becomes entrained into the granular jet. This motion is particularly descriptive as it shows a small downward displacement for approximately 50 ms as the sphere passes, then a change in the direction of motion as it becomes entrained into the jet, thereafter exhibiting a ballistic profile, reaching a maximum height of 80 mm above the bed surface. Based upon the total vertical displacement $\Delta z \approx 90$ mm of this particle, we estimate the initial speed of this particle

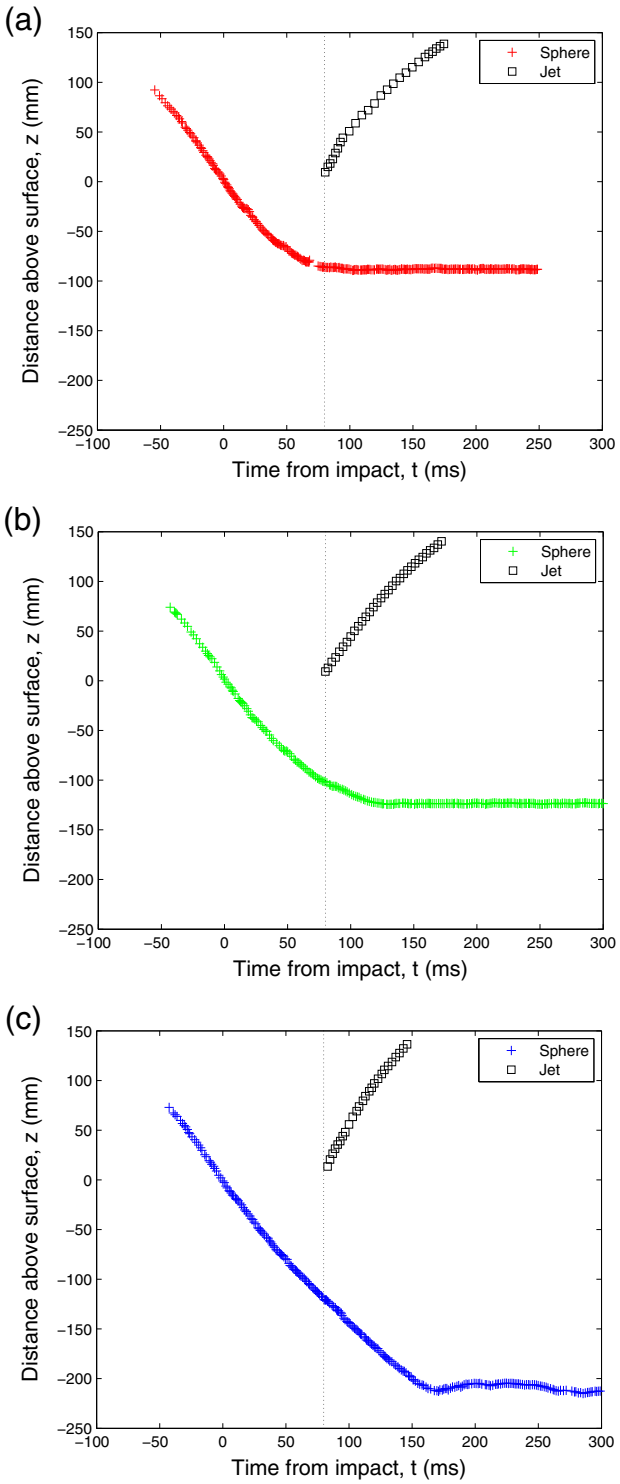

Fig. 3. Jet height and sphere depth vs. time from impact for the (a) $\phi = 0.62$, (b) $\phi = 0.6$ and (c) $\phi = 0.55$. $V_0 = 1.81$ m/s, $D_0 = 20$ mm, $Fr = 34$. The vertical dashed line in each plot represents the approximate time ($t_{jet} \approx 80$ ms) that the tip of the jet emerges above the initial surface level.

as $V_{i.particle} \approx \sqrt{2g\Delta z} = 1.33$ m/s, which is slightly lower than the speed of the tip of the jets measured in Fig. 5. From this, we conclude that the particle was entrained into the mid-portion of the jet. The particle then reaches a final position approximately 200 mm above the bottom of the bed, close to the initial height near the surface of the bed. Clearly, there is some degree of scatter amongst these data points, highlighting

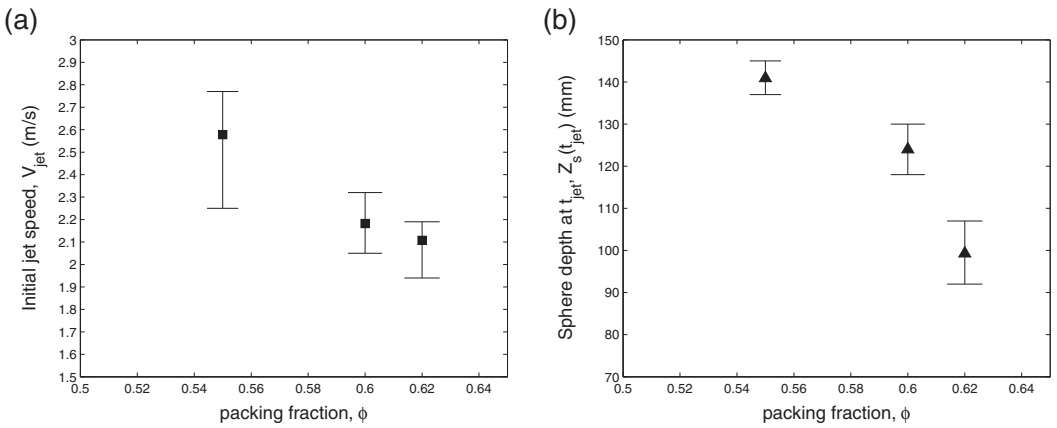

Fig. 4. (a) Initial jet speeds, V_{jet}, over 10-frame interval after emergence above initial bed surface and (b) sphere depth below bed surface when jet emerges, $Z_s(t = t_{jet})$, both plotted against initial bed packing fraction, ϕ.

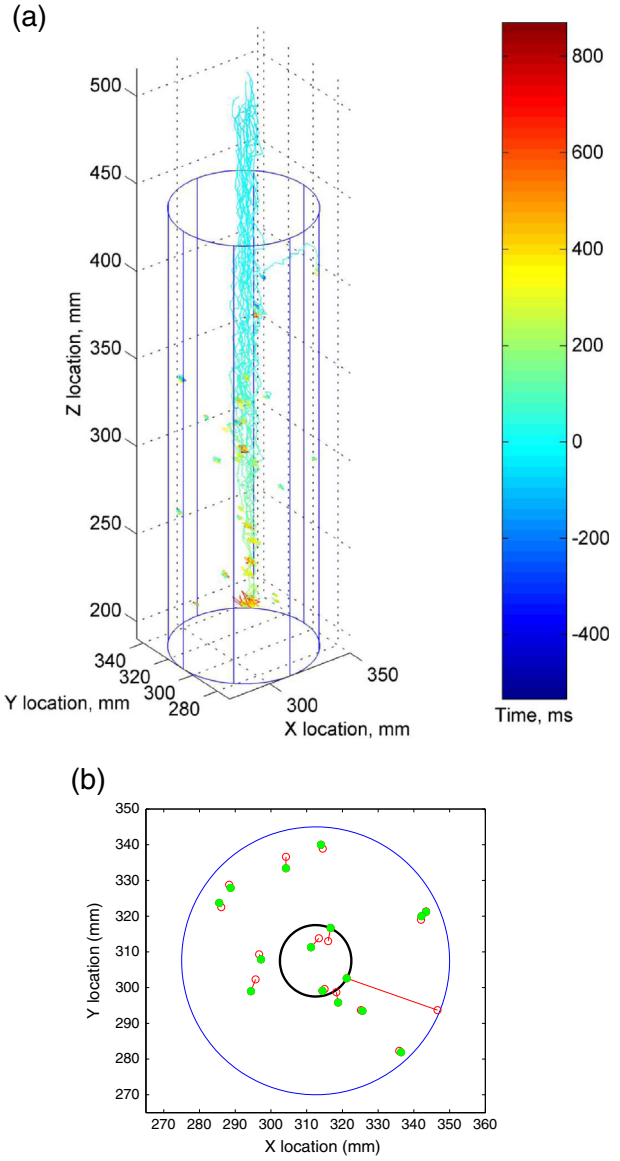

Fig. 5. Location versus time for particles in a low-packing fraction bed ($\phi = 0.55$). The color bar indicates time in milliseconds from impact. The displacement in the $x - y$ plane of the same particles is shown in (b), where green indicates initial position and red indicates final position. (For interpretation of the references to colour in this figure legend, the reader is referred to the web version of this article.)

the need for further refinements to the PEPT technique and post-acquisition analysis, especially with tracking multiple particles simultaneously. However, with ongoing efforts [2], it is anticipated that a more thorough description of the origins and dynamics of the granular jet, and other impact-related phenomena can be obtained.

4. Concluding remarks

We have performed an experimental study of sphere impact onto granular beds. Using tracers attached to the impacting sphere and tracers in the bed, we have simultaneously obtained the time-resolved sphere trajectory and bed particle motion. In some cases, we tracked particles which become entrained into the granular jet which can arise following the collapse of the cavity in the bed.

Due to the robust nature and ever-improving accuracy of the experimental technique, PEPT may prove itself advantageous over other techniques such as conventional video imaging and X-ray imaging for other granular flow configurations. In particular, individual particle motion in fully three-dimensional flows can now be readily obtained. Refinements to the experiments reported herein are the subject of ongoing work.

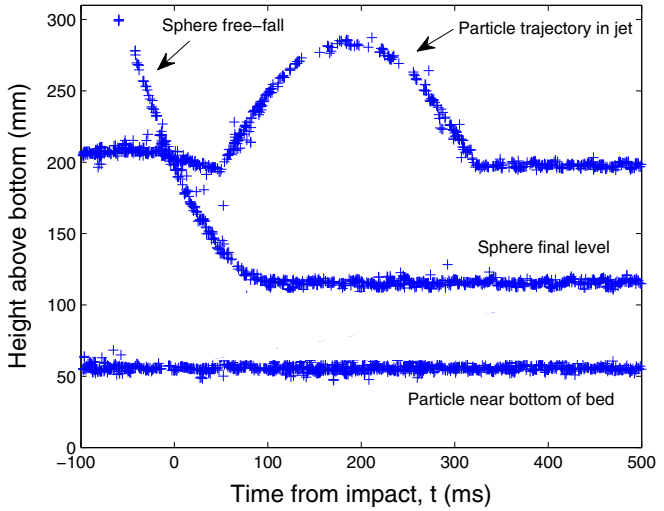

Fig. 6. Combined trajectories of the sphere, a particle entrained into the granular jet, and a particle residing near the bottom of the bed.

Acknowledgements

This work was partially supported by an Academic Excellence Alliance grant awarded by the KAUST Office of Competitive Research Funds number 7000000024. The experimental work was conducted whilst J.O.M. was on a research visit to the University of Birmingham. The authors thank Andy Ingram for the assistance and advice with the experimental setup, and Thomas Leadbeater, Joseph Gargiuli and Dave Parker for assisting with the experiments and analysis.

References

[1] D.R. Dowling, T.R. Dowling, Scaling of impact craters in unconsolidated granular materials, Am. J. Phys. 81 (2013) 875.
[2] T.W. Leadbeater, D.J. Parker, J. Gargiuli, Characterization of the latest Birmingham modular positron camera, Meas. Sci. Technol. 22 (2011) 104017.
[3] D. Lohse, R. Rauhe, R. Bergmann, D. van der Meer, Granular physics: creating a dry variety of quicksand, Nature 432 (2004) 689.
[4] J.O. Marston, E.-Q. Li, S.T. Thoroddsen, Evolution of fluid-like granular ejectas generated by sphere impact, J. Fluid Mech. 704 (2012) 5–36.
[5] J.O. Marston, I.U. Vakarelski, S.T. Thoroddsen, Sphere impact and penetration into wet sand, Phys. Rev. E. 86 (2012) 020301(R).
[6] J.O. Marston, J.P.K. Seville, Y.-V. Cheun, A. Ingram, S.P. Decent, M.J.H. Simmons, Effect of packing fraction on granular jetting from solid sphere entry into aerated and fluidized beds, Phys. Fluids 20 (2008) 023301.
[7] F. Pacheco-Vazquez, G.A. Caballero-Robledo, J.M. Solano-Altamirano, E. Altshuler, A.J. Batista-Leyva, J.C. Ruiz-Suarez, Infinite penetration of a projectile into a granular medium, Phys. Rev. Lett. 106 (2011) 218001.
[8] D.J. Parker, T.W. Leadbeater, X. Fan, M.N. Hausard, A. Ingram, Z. Yang, Positron imaging techniques for process engineering: recent developments at Birmingham, Meas. Sci. Technol. 19 (2008) 094004.
[9] J.R. Royer, E.I. Corwin, A. Flior, M.-L. Cordero, M.L. River, P.J. Eng, J.M. Jaeger, Formation of granular jets observed by high-speed X-ray radiography, Nat. Phys. 1 (2005) 164–167.
[10] J.R. Royer, B. Conyers, E.I. Corwin, P.J. Eng, H.M. Jaeger, The role of interstitial gas in determining the impact response of granular bed, Europhys. Lett. 93 (2011) 28008.
[11] S.T. Thoroddsen, A.Q. Shen, Granular jets, Phys. Fluids 13 (2001) 4–6.
[12] R.D. Wildman, C.M. Hrenya, J.M. Huntley, T.W. Leadbeater, D.J. Parker, Experimental determination of temperature profiles in a sheared granular bed containing two and three sizes of particles, Granul. Matter 14 (2012) 215–220.
[13] H. Katsuragi, D.J. Durian, Unified force law for granular impact cratering, Nature Physics 3 (6) (2007) 420–423.
[14] D.I. Goldman, P.B. Umbhanhowar, Scaling and Dynmaics of sphere and disk impact into granular media, Phys. Rev. E 77 (2008) 021308.